Global and Planetary Change
September 2023, Volume 228, Pages 104194 (15p.)
https://doi.org/10.1016/j.gloplacha.2023.104194 https://archimer.ifremer.fr/doc/00847/95904/

Hydrodynamical impact of the July 2022 'Code Red' distant mega-swell on Apataki Atoll, Tuamotu Archipelago

Andréfouët Serge [1, 2, *], Bruyère Oriane [4], Liao Vetea [3], Le Gendre Romain [4]

[1] IRD, UMR 9220 ENTROPIE, Institut de Recherche pour le Développement, Univ de la Réunion, IFREMER, Univ. Nouvelle-Calédonie, CNRS, BPA5, 98948 Noumea, New Caledonia
[2] IRD, UMR-9220 ENTROPIE, Institut de Recherche pour le Développement, Université de la Réunion, IFREMER, CNRS, Université de la Nouvelle-Calédonie, BP 49 Vairao, Tahiti, French Polynesia
[3] Direction des Ressources Marines, BP 20, 98713 Papeete, French Polynesia
[4] Ifremer, UMR 9220 ENTROPIE, IRD, Univ. Réunion, IFREMER, Univ. Nouvelle-Calédonie, CNRS, BP 32078, 98897 Nouméa Cedex, New Caledonia

* Corresponding author : Serge Andréfouët, email address : serge.andrefouet@ird.fr

Abstract :

Distant swells generated by storms in the high latitudes (>40°) can impact islands and atolls of the Pacific Ocean far from their genesis locations. While common, they can also occasionally generate very high wave height (>5 m) at high period (>16 s) during several days. These rare mega-swells can damage distant human infrastructures in tropical islands by direct wave impacts, but also by the extreme elevation of the sea level in lagoons exposed to the incoming swell. The lagoon surge, and land flooding, resulting from these events can be catastrophic, especially for low-lying atolls. In July 2022, the hydrodynamic conditions during the third highest energy southern mega-swell of distant origin (55°S-150°W) impacting French Polynesia since 1996 could be monitored real time with an array of sensors (pressure, acoustic Doppler current profilers, temperature) previously deployed to study the physical environment of black pearl farms in Apataki Atoll (15.45°S, 146.35°W), a semi-open atoll of the Tuamotu Archipelago. This was a unique opportunity to characterize for the first time the hydrodynamics conditions before, during and after a mega-swell with measurements of lagoon and ocean water levels, incoming wave heights and periods on the oceanic forereef, current speeds and directions along the atoll rims and in the deep passes. The array of available sensors provided a real time spatial view of the transient conditions that the atoll experimented during the mega-swell event, that can complement the more traditional assessment carried out after similar events using sedimentologic and geomorphologic evidences. While the degree of protection offered by atolls in the south of Apataki have limited the impact, the significant wave height (up to 4.2 m), flows in the passes (with up to 6.4 knots outgoing currents) and a 0.5 m surge above the average lagoon level characterize a major event. Other atolls (e.g., Makemo) have experienced higher surges in similar events in 1996 and 2011, which confirms that assessment of risks induced by mega-swells should be specific to each atoll according to its position, exposure, geomorphology and the settlement of human infrastructures.

Highlights

► Pacific Ocean atolls are exposed and vulnerable to distant mega-swells. ► Hydrodynamic conditions in atolls during mega-swells are poorly known. ► In July 2022, an array of sensors in Apataki atoll captured these conditions. ► Wave, surge & currents are described before, during & after the event. ► Surge and damages were limited for Apataki, but remain highly atoll-dependent.

Keywords : Pearl farming, hoa, lagoon, wave, WaveWatch III, sea level, surge, distant source swell

Introduction

Atolls can be defined as a reef rim surrounding a hydrodynamically closed to semi-closed shallow lagoon. Reef islands can be found on the rim, sitting on antecedent reef platforms. They result from sediment deposit, built up and cementation brought from the ocean. These landforms are seldom more than a few meters high (Smithers 2011), and atolls and their inhabitants' future are highly vulnerable to the local future hydrodynamic regimes and in particular oceanic incident waves and sea level variations. However, short episodes of high waves are much more efficient in fast removing or accumulating layers of sediments than sea level rise (Tuck et al. 2019), and there are sometimes confusions when pointing to factors responsible to changes in reef island coastlines. Nowadays, sea level rise will be often quickly pointed at as the cause of changes by general public, managers and media, while the changes may be better explained by a storm or an overlooked unusually high energy wave season (Griggs and Reguero 2021). While, there has been much debate on studies on sea level rise due to global warming and its implications for reef islands worldwide (Yamano et al. 2007, Andréfouët et al. 2015, Ford and Kench 2015, Kench et al. 2018), the impact of waves is less put forward despite a significant body of work (see Munk and Sargent 1948, Maragos et al. 1973, Kench et al. 2006, Callaghan et al. 2006, Smithers and Hoeke 2014, Pedreros et al. 2018, Tuck et al. 2019, Canavesio 2019, or Duvat et al. 2020a among others). Among these investigations, the conditions during rare very high waves (Significant Wave Height, Hsig, >5m) are poorly characterized (Kench et al. 2008). These high waves can be generated by high latitude distant storms, tropical cyclones, and tsunamis. Hydrodynamical conditions during all these events are difficult to measure, since they are not necessarily easily predictable long time in advance (one week to few days at best), and sensors deployment takes time to be organized for remote places in case of a coming event. Moreover, during the event itself, the conditions on the reefs and islands can be quite dangerous and impractical for a man-based survey. Therefore, the intensity of such events can be captured in real time *in situ* only rather opportunistically, in the case of automatic recording sensors already moored in relevant places well before the high wave event. Among these distant storms, tropical cyclones and tsunamis, the latter are very short high energy event lasting less than an hour at a given place (Purkis et al. 2023). Conversely, distant swells and tropical cyclones generate high energy swell that can impact a location for few days. Cyclones are high energy event, but their sphere of influence is nevertheless limited to a couple of thousands of kilometers (Laurent and Varney 2009). In a given tropical region, cyclones can occur frequently like in the West Pacific or much more rarely, like in the Central-East Pacific. Low atmospheric pressure during cyclones also contribute to a local higher sea level that enhance the wave damage potential. Conversely, distant swells born from storms in the middle to high latitudes (in the 35-60° belt of the austral and septentrional oceans) are more

common throughout the Pacific Ocean, including in the Central-East Pacific. They include high to mega-swell episodes characterized by large fetch, high wave heights and very long periods (>16s). They are threats lasting few days and able to cross an ocean. These distant exceptionally rare swells have generated much damages (flooding, destruction of houses and infrastructures, etc.) in the island archipelagoes of the Pacific Ocean (Hoeke et al. 2013, Canavesio 2019, Wandres et al. 2020,) and they deserve better characterization. This is the focus of this study.

The Tuamotu atoll lagoons in French Polynesia have been extensively studied recently. In the context of black pearl farming for instance, numerous biophysical topics were addressed, including physical oceanography, as well as rim and lagoon hydrodynamics (Dumas et al. 2012, Dutheil et al. 2020, 2021; Aucan et al. 2021, Andréfouët et al. 2022, Le Gendre et al. in prep.). The Tuamotu is the largest atoll-only archipelago worldwide, with 77 atolls, among which 20 are pearl farming atolls representing 74% of the total farming area in French Polynesia. Most recent *in situ* pearl farming-related work have mostly focused on four atolls only, namely Ahe, Takaroa, Raroia and Takapoto. Besides Ahe studied in 2008-2009 (Dumas et al. 2012) and 2013 (Andréfouët 2013), these atolls have been the subject of physical oceanography sensors deployment since 2018 (from 3 months to nearly one year-long leg), although the covid pandemic slowed down field work in 2020-2021. However, in July 2022, the MALIS3 oceanographic cruise on board R/V ALIS was scheduled to initiate the study of Apataki Atoll, a large pearl farming atoll of the central-west Tuamotu. As such, one of the main goal was to install for about one month a total of five Acoustic Doppler Current Profilers (ADCP) in strategic locations to complement an array of pressure and temperature sensors already deployed since the end of April 2022. During this cruise, we had the opportunity to monitor the atoll conditions during what is perceived as the third mega-swell of distant origin hitting the Tuamotu in the last 25 years (Canavasio 2019). This was the second time in history after August 2011 that the local Météo-France weather service released a 'Code Red' warning, in practice forbidding all marine and coastal activities in islands subjected to the incoming swell.

Previously, high energy wave events in the Tuamotu have been indirectly studied through sedimentary and geomorphologic evidences left on reef islands, such as mega-blocs that are massive pieces of the reef framework tore out from the slope and transported on the nearby reef flats, conglomerate platforms or land (Bourrouilh-Lejan and Tallandier 1985, Canavesio 2015, Lau et al. 2016, Montaggioni et al. 2018). Another source of information is the local memory, and interviews with inhabitants may provide some clues to identify surge levels and locations of new or inactive water spillways becoming active at the time of recent event (Magnan et al. 2018, Canavesio 2019). The Météo-France office based in Tahiti has also examined the trajectory and characteristics of historical cyclones (Laurent and Varney 2014). The wave regime of Tuamotu atolls has been recently

revisited (Dutheil et al. 2021), but by definition regimes do not represent rare and extreme short-term events that require *in situ* work for a better understanding of their hydrodynamical effects. None of these studies could rely on *in situ* lagoon or rim measurements concurrent to the swell events. Only meso-scale oceanographic and atmospheric models and selected satellite altimetry data for the recent period (1992-present) are available to describe the phenomenon. For instance, Canavesio (2019) could analyze the significant wave heights and periods of the July 1996 and August 2011 mega-swells by using WaveWatch III (WW3) hindcast model data (Tolman 2009). The applied value for management of these studies are nevertheless immediate, and Canavasio (2019) for instance eventually points out to urban planning decisions that may indirectly increase the surge impact, and damage further human made infrastructures.

For semi-closed to semi-open atolls (Andréfouët et al. 2022), the hydrodynamical mechanisms and features by which atolls and islands on top of the atoll rims are impacted by distant mega-swell event can be explained qualitatively here. First, semi-closed atolls are atolls for which most sections of the rim are shallow or intertidal reef flats (called *hoa* in the Tuamotu), and at least one section of the reef is deep, marking the presence of a pass. The degree of aperture of the atoll is defined by the proportion of the open reef flat total length relative to the total perimeter of the atoll (Andréfouët et al. 2001, Andréfouët et al. 2022). The circulation between the lagoon and the ocean is function of the differences of water level between them. These can vary periodically with tide, and more randomly due to other meso-scale oceanographic features and meteorological events passing by factors such as incoming distant swells, cyclones, oceanic eddies, large-scale currents, and local wind waves. In the semi-closed to semi-open atolls, lagoon water level is neither equal to the setup on the reef rim nor equal to the open ocean water level. Instead, lagoon water level results from a combination of tidal elevation driven by ebb and flushing through reef passes that can be several kilometers away, and by wave driven inflows and outflows occurring at many other places around the atoll. When incident waves break on the rim crest, they drive the wave setup in the breaking zone as well as the across-reef flow downstream of the breaking zone (Tartinville and Rancher 2000, Monismith 2017, Aucan et al. 2021). The more the length of *hoa* exposed to the incoming swells and the higher the waves, the more the inflows create a rapid and abnormal high lagoon elevation. The speed and amplitude of the lagoon elevation, and the resulting differences of levels with the ocean, will be also a function of the outgoing flows. Outgoing flows can occur through the passes, and through outgoing *hoa* that may be present away from the wave impact zones. The smaller these outgoing openings the higher the lagoon elevation. Eventually, how an atoll will be impacted depends on all these factors, without forgetting the topographic elevation of the reef islands themselves. Here, we are interested

by understanding better the functioning of the *hoa*, the passes, and the resulting lagoon elevation during a distant mega-swell event.

To follow the study by Canavesio (2019) on the impact of distant swells on Makemo Atoll in the central Tuamotu (Figure 1), and increase our knowledge on the impact of these phenomena, the objective of this paper is thus to provide for the first time an array of hydrodynamic measurements on one atoll (Apataki) during a distant mega-swell event, in particular current measurements in the deep passes and shallow rim reef flats, as well as the lagoon levels. Significant wave height outside the atoll were also measured. The available array of sensors also allows for the first time discussing the spatial heterogeneity of hydrodynamic responses occurring throughout the lagoon and its borders (passes and reef flats). We highlight the implications of these measurements in the context of Tuamotu atolls population resilience, but also pearl farming, which is at the center of our research on atolls since 2004 (Andréfouët et al. 2006).

Material and Methods

Study site

Apataki is a very large (706 km^2) atoll of the central west Tuamotu (Figure 1) centered by 15.45°S, 146.35°W. It is classified as semi-open, considering the presence of two deep passages on the western side of the atoll, and numerous *hoa* mostly on its south and western side. The two passes (named Tehere in the north and Pakaka in the south) reach a maximum depth of about 30m in their central section. Elsewhere, the atoll is closed by a continuous rim covered by vegetation for half of its contour. The shallow *hoa* allow for water exchanges between the lagoon and the ocean. *Hoa* morphologies can be different from one side of the atoll to the other, and they are wider and deeper in the south than in the west sides of the atoll. They are found in the south where they form a continuous reef flat closed by sand banks, and in the west, where they are intersected by large reef islands (locally named *motu*). The north and east sides of the atoll are completely closed by vegetated land, except for a few narrow *hoa*. The bathymetry of the lagoon is unknown for most of its extent, but selected multibeam bathymetric measurements made by R/V Alis when crossing the lagoon suggest a maximum depth of about 50m (Andréfouët and Le Gendre 2023, unpublished data).

Apataki lies just north of three atolls (Kaukura, Toau and Niau), that may completely block an incident swell depending on its direction (Andréfouët et al. 2012). The most exposed conditions for Apataki would be during south or south-southeast swells (Figure 1).

The 2019 census reported 442 inhabitants in Apataki Atoll, mostly living in the village bordering the south pass. Apataki is an important pearl farming atoll, with several concessions covering nearly 800

ha. The level of existing scientific knowledge relevant for pearl farming was however virtually nil before our July 2022 survey. Other economic activities include fishing (with 34 registered fish traps in 2019), coprah production (67 tons in 2019), and a small tourism activity, limited by a lack of airport with an airstrip long enough to receive regional commercial planes. Cargo ships from Tahiti stop almost every week on this atoll.

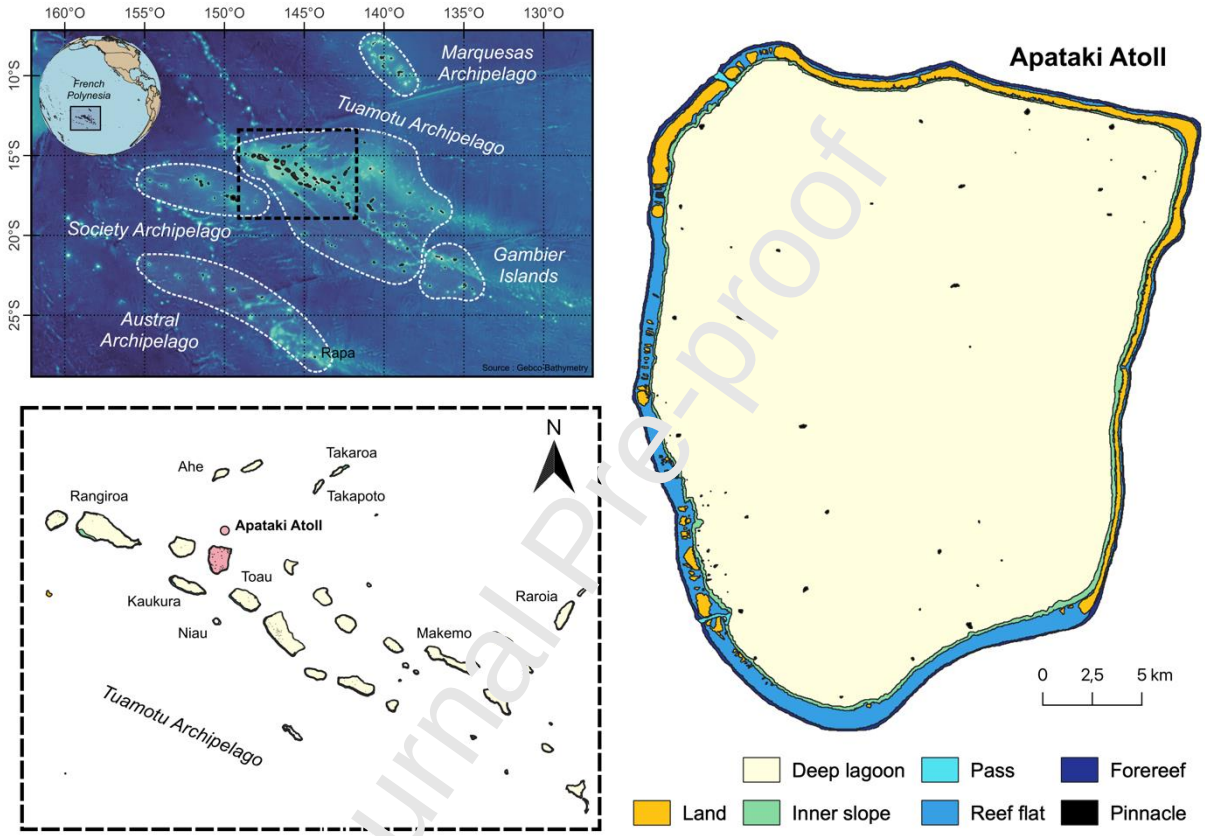

Figure 1: Map of French Polynesia, and location of Apataki Atoll in the Tuamotu Archipelago. The geomorphological map on the lower right shows the locations of reef flats (light blue) where oceanic water can be driven into the lagoon due to action of incoming waves and rising tides.

The July 2022 mega-swell

According to Météo-France (Roy et al. 2022), the episode was born from a vast low-pressure system (minimum 946hPa) at 55°S-150°W (or 3000km in the south-southwest of Rapa Island, the most southern French Polynesia Island). This system was almost stationary due to the high-pressure system close to Easter Island in the East. Pressure gradient was also constrained by the Kermadec anticyclone in the west. Winds with speed >35 knots were blowing 1600 km from the center, creating a very wide fetch zone. Once established, swell periods were estimated to be almost 17s (Roy et al. 2022). WW3 numerical model is in agreement with these values, with periods peaking the 14th at

noon UTC time at 16.77s. Météo-France, through the WAVERYS model, reports a maximum Hsig in the central-west Tuamotu of 4.6 m. Propagation of the swell and Hsig according to WW3 is shown in Figure 2. The swell propagated from a south-southwest direction.

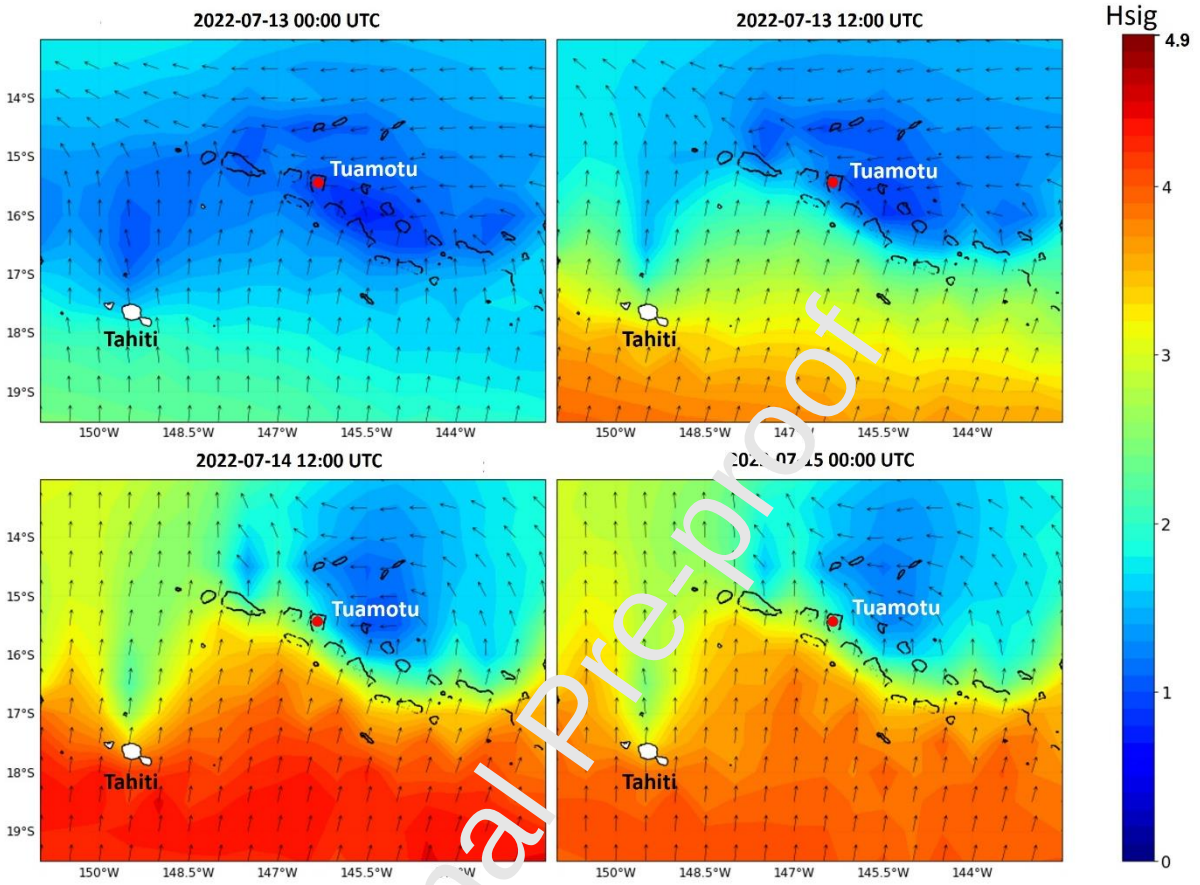

Figure 2: Significant wave height (Hsig) in the Tahiti Island and Western Tuamotu region, from 13th July to 15th July 2022 according to WaveWatch III (WW3) 30' resolution model. The red dot indicates the position of Apataki Atoll. In addition to Hsig shown here, the WW3 maximum swell period for this event on the space and time referential corresponding to the figure was 16.7 seconds (14th July at noon UTC).

The barriers to swell propagation formed by Tahiti Island and the Tuamotu Archipelago are clearly visible on WW3 data at this resolution (30'). Considering the position of Apataki relative to nearby atolls (Figure 1), it is certain that Kaukura, Niau and possibly Toau (Figure 1) have filtered out part of the incident signal (Andréfouët et al. 2012), and thus the incoming swell in Apataki was not at the peak of its energy compared to the south of Kaukura or Niau for instance (Figure 1). Nevertheless, the open channel between Kaukura and Toau and the main swell direction (south-southwest) explains that the south rim of Apataki has been directly impacted by the event.

Sensor deployment

Apataki Atoll was equipped with autonomous instruments over 3 months, delimited in two legs (Table 1). First Leg, from 20/04/2022 to 01/07/2022, the forereef and lagoon were equipped with pressure/temperature sensors (RBRduet T.D) to record water elevation and surge variation inside the lagoon (stations L01-L02-L03-L04-L05, Figure 3, Table 1). Second, reef flats of the south rim were equipped with two shallow water Nortek Aquadopp sensors, moored at 2 to 3m depth (Stations AQ1 and AQ2) downstream from two RBRduet T.D pressure/temperature sensors positioned on the forereef at 10 meter deep to deduce the incident waves (stations O01 and O02). This set up allows to assess the relationship between incident waves and incoming current speeds in the reef flat (as Aucan et al. 2021 demonstrated for Raroia Atoll – central Tuamotu). Then, starting on 01/07/2022, the second leg maintained the initial deployment but added one RBRduet T.D at station L06, and three Teledyne Sentinel ADCP: one V50 in the middle of each pass (stations P01 and P03), and one V20 in the lagoon within the jet of the south pass to measure current speed and direction over the water column (Station P02, Figure 3, Table 1). The position, depth and acquisition frequency of each sensor are provided in Table 1. Due to the size of the lagoon, not all instruments could be deployed or retrieved the same day, hence some sensors started to record up to 2 days after the first one. Sensors in the north (L6 and P03) started 04 and 05/07/2022 respectively. By 29/07/2022 all sensors were retrieved. The R/V ALIS provided the logistical support during the so-called MALIS3 campaign.

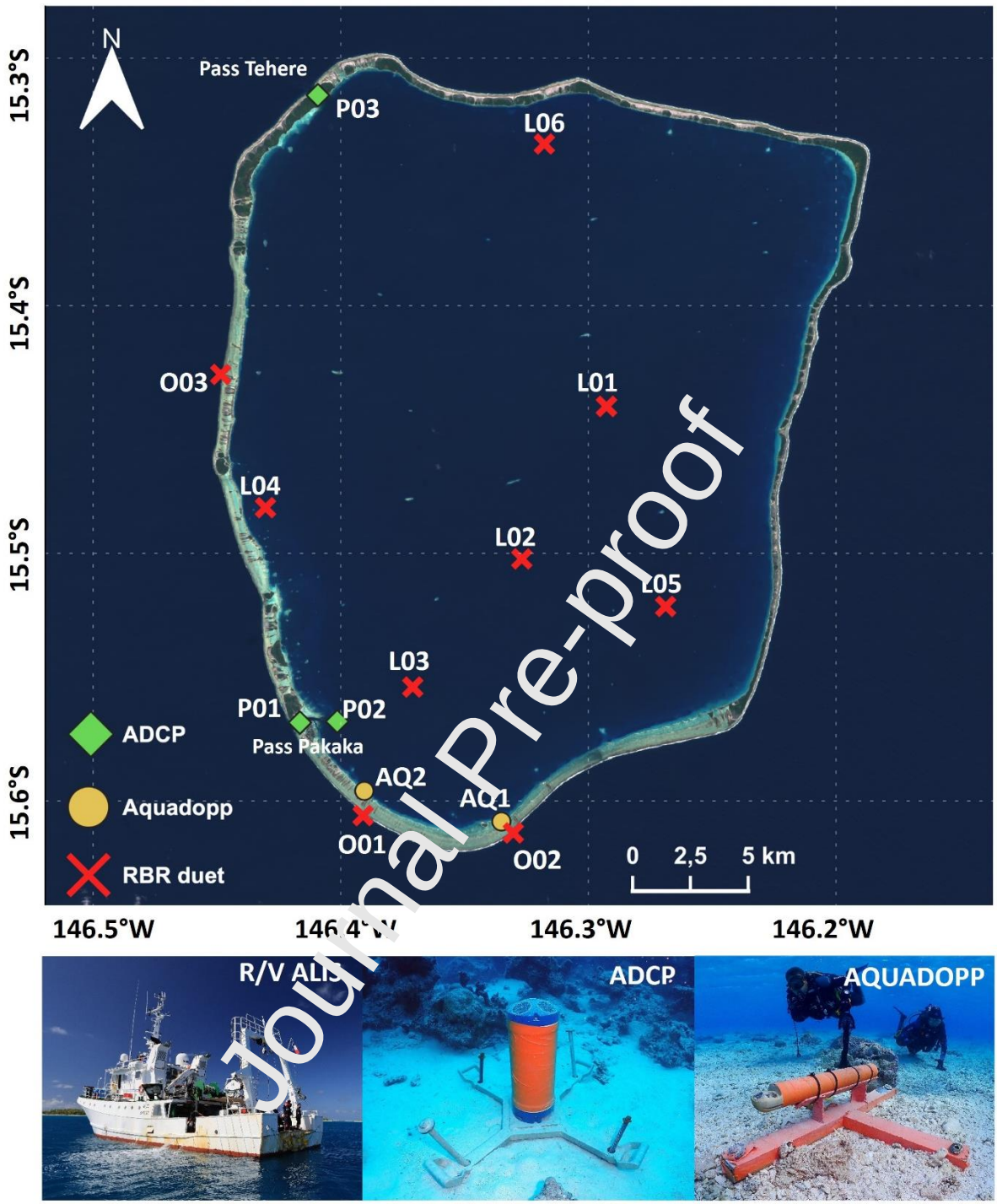

Figure 3: Top panel: map of current meters (deep ADCP and shallow Aquadopp ADCP), and pressure (RBRduet T.D) sensors deployed in Apataki. Bottom: The R/V ALIS was used for the second leg operations, with illustrations of the current meter instruments moored in P02 and AQ2 stations. Background satellite image from Sentinel-2 imagery.

Table 1: Description of deployed loggers in Apataki between April 2022 and late July 2022. Other sensors were deployed but are not relevant for this study and are not shown here. T/P= Temperature/Pressure.

Station	Latitude (S)	Longitude (W)	Instrument	Raw parameters	Freq	Depth	Processed parameters	Legs
O01	-15.605983	-146.39095	RBRduet T.D	T/P	1"	10m	Temperature – wave height & period – water level	1-2
O02	-15.613003	-146.330261	RBRduet T.D	T/P	1"	12m	Temperature – wave height & period – water level	1-2
O03	-15.427796	-146.448461	RBRduet T.D	T/P	1"	7m	Temperature – wave height & period – water level	1-2
AQ1	-15.608373	-146.335086	Nortek Aquadopp	Currents –T/P	10'	2m	Temperature – currents speed & direction – water level	1,2
AQ2	-15.596022	-146.390457	Nortek Aquadopp	Currents –T/P	10'	2m	Temperature – currents speed & direction – water level	1,2
P01	-15.568417	-146.416472	Sentinel ADCP V50	Currents –T/P	10'	27m	Temperature – currents speed & direction – water level	2
P02	-15.567935	-146.401393	Sentinel ADCP V20	Currents –T/P	10'	21m	Temperature – currents speed & direction – water level	2
P03	-15.31504	-146.40919	Sentinel ADCP V50	Currents –T/P	10'	31m	Temperature – currents speed & direction – water level	2
L01	-15.440699	-146.292631	RBRduet T.D	T/P	1"	12m	Temperature – wave height & period – water level	1-2
L02	-15.502053	-146.326799	RBRduet T.D	T/P	1"	12m	Temperature – wave height & period – water level	1-2
L03	-15.502053	-146.326799	RBRduet T.D	T/P	1"	12m	Temperature – wave height & period – water level	1-2
L04	-15.502053	-146.326799	RBRduet T.D	T/P	1"	12m	Temperature – wave height & period – water level	1-2
L05	-15.521516	-146.268736	RBRduet T.D	T/P	1"	9m	Temperature – wave height & period – water level	1-2
L06	-15.33485	-146.31786	RBRduet T.D	T/P	1"	10m	Temperature – wave height & period – water level	2

After sensors were retrieved and data downloaded, data processing steps were necessary on pressure data recorded with RBRduet T.D loggers to acquire wave parameters (Bruyère et al. 2022). Pressure data were corrected from a constant atmospheric pressure (101 325 bar), then values were filtered using the Fourier transform to apply the linear wave theory (method used in Aucan et al. 2017) to obtain a water elevation time series at every minute, and waves parameters (significant wave height, wave period, etc.) at hourly frequency. Water elevation was corrected from the mean sea level corresponding to the averaged time series depth. Finally, ADCP velocities and directions data were filtered to avoid contaminated surface cells.

Depending on the temporal scale of analysis, filtering is applied to remove the effects of tide at daily scale. Water elevations and currents data can be filtered from tidal effects by applying Demerliac tide filter (Demerliac 1974). The tidal signal is removed using a 72 hours windows. Depending on the analysis, the current velocity data (Aquadopp and Sentinel ADCPs), tide-filtered or not, can be projected on the main current direction axis.

***Wave* versus *current velocities in* hoa**

The impact of the mega-swell on the atoll will be dependent on the lagoon level elevation, and lagoon level elevation will depend on the south swell hitting the south rim. Although a precise

estimation of the wave-driven flows and lagoon renewal is beyond the scope of the present study, it is important to confirm the water pathways and the magnitude of the exchanges relative to the lagoon level elevation. For this, we investigate the currents in the *hoa* following a methodology already implemented for Raroia Atoll (Aucan et al. 2021). In doing so, we first check if the Raroia formulations and results remain also valid for Apataki and during a high wave event.

The hydrodynamic sampling strategy had two shallow Aquadopp ADCP in two differently exposed *hoa* (southwest and southeast) of the south rim sector, each paired with one RBRduet T.D pressure/temperature sensor moored on the oceanic reef slope in order to measure the effects of wave height on current velocities in the *hoa* (Figure 2). Aucan et al. (2021) presented the same strategy for Raroia Atoll. Dumas et al. (2012) similarly studied another atoll (Ahe Atoll). Raroia, Ahe and Apataki can be compared as they all have passes and sections of active *hoa,* although Apataki and Raroia are much more open than Ahe. In these atolls, the oceanic tide is not synchronous with the lagoon tide, and a phase lag of 2 hours in Ahe and up to 4 hours in Raroia can occur (Dumas et al. 2012, Aucan et al. 2021). Lagoon water levels are therefore also not phased with the ocean sea level. Indeed, the water level downstream of the surf zone, across the *hoa* is controlled by the tide, and by the lagoon wide return flows through the reef pass. Therefore, it is not possible, with our bottom-mounted RBR sensors quite far apart, to recalibrate exactly the differences between the lagoon and oceanic levels at any time. This drawback is compensated here, as in Aucan et al. (2021), by using the variations of water level for the lagoon and the ocean around their respective time-average.

The key forcing parameters of an across-rim flow are the significant wave height H_{sig} and wave period *Tm01*, or the breaking wave height (H_b) which is $Hb = H_{sig}^{4/5} Tm01^{2/5}$ (Caldwell and Aucan, 2007; Hench et al. 2008) for a shore-normal incoming wave.

To estimate water speed in the *hoa* that is only due to the waves (e.g., the daily-averaged current), we use a simple model with the daily average (e.g. de-tided) values as:

$$U_{daily} = AH_b + C \quad \textit{(Equation 1)}$$

where U_{daily} is the daily current measured in the *hoa* (average on the vertical) and projected here against the mean current direction. A and C are constants.

To simulate hourly currents in the *hoa*, thus dependent on both tidal elevation changes and wave height, we included a pressure gradient term and a constant B:

$$U_{hourly} = AH_b + B\left[\left(h_{ocean} - \overline{h_{ocean}}\right) - \left(h_{lagoon} - \overline{h_{lagoon}}\right)\right] + C \quad \textit{(Equation 2)}$$

where h_{ocean} and h_{lagoon} are the sea-level height outside the reef and inside the lagoon respectively. The overbar designates the time-averaged quantities. A, B and C are constants to estimate using field

data and a multi-regressions analysis. As explained in Aucan et al. (2021), the first term represents the effect of waves, the second term represents the effect of water level difference between ocean and lagoon, and the third is a constant.

To model current speed *vs* H_{sig} at daily and hourly scales, we first used the mean models coefficients quantified by Aucan et al. (2021) for three *hoa* in Raroia. Then, using the formulation from equations 1 and 2, we also computed a new relationship optimized for each of the Apataki *hoa* using data from both Leg 1 and Leg 2 to use a maximum of the available data. This provides a test of the robustness of Aucan et al. (2021) findings. We also assessed the robustness of the statistical relationships in high wave conditions, which were not met in Raroia, by including, or excluding the mega-swell event.

Meteorological data

Meteorological data are provided from ERA5 reanalysis atmospherical model (global model at 0.25° resolution, or ~27.3 km resolution) giving U and V component of wind at 10m above the surface at hourly time step. These parameters have been extracted at one location into Apataki Atoll (146°20'7.746'' W; 15°27'4.032'' S). Wind speed and direction of the horizontal 10m wind are deduced from U, V parameters.

Results

Tides and lagoon-ocean phases

The Figure 4 illustrates the variations of the tide signal in the ocean *vs* the lagoon in Station L03 (all lagoonal stations reacted *quasi* exactly the same), before, during and after the mega-swell event. The lag between ocean and lagoon tides was two hours before the event, then it increased the 13th July until peaking at up to 5 hours the 14th July 0.0 AM UTC, when the swell was at highest, before progressively decreasing in parallel to the swell and returning back to a 2-hour lag the 15th of July, 1.0 AM UTC. The differences of amplitude between ocean and tides are variable, but it was maximal during the mega-swell event after the end of 13th July, with a strong distortion of the lagoonal tides (Figure 4).

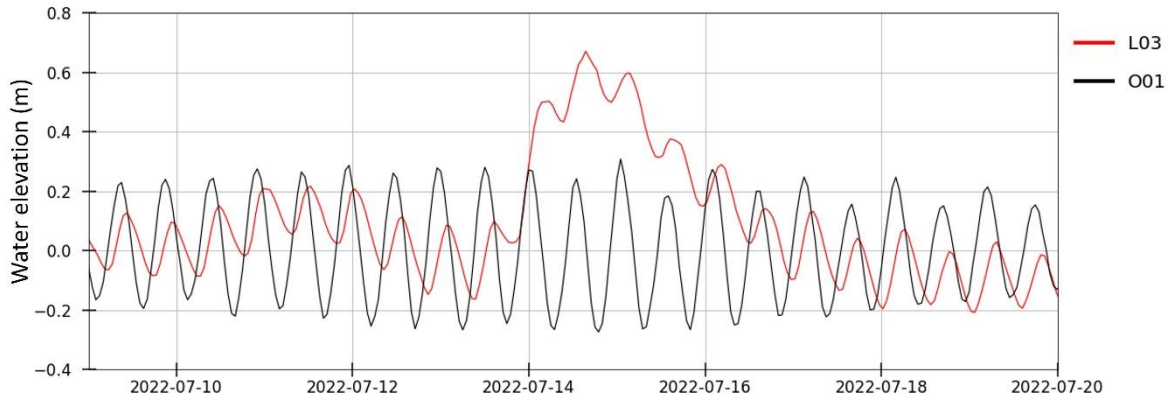

Figure 4: Tide differences between the ocean (station O01) and inside the lagoon (L03), before, during and after the mega-swell event. The time lag between oceanic and lagoonal tides is visible as the time differences between two adjacent oceanic and lagoonal tide peaks. The tidal amplitude is also much reduced in the lagoon compared to the ocean in normal conditions.

From these observations, we conclude that the tide is still transferred into the lagoon during the mega-swell event, but with a higher delay than in normal conditions. The large difference in levels between the lagoon and ocean (Figure 4) can be attributed to the wave pumping into the lagoon.

Oceanic waves and lagoon surges

Figure 5 presents for the Leg 2 survey: i) the ERA5 wind speeds and directions at hourly frequency ii) the significant wave height (Hsig) and the wave period (TM01, also commonly named P) from the three pressure sensors moored on differently exposed forereefs, iii) the surge for each of the six lagoonal pressure sensors.

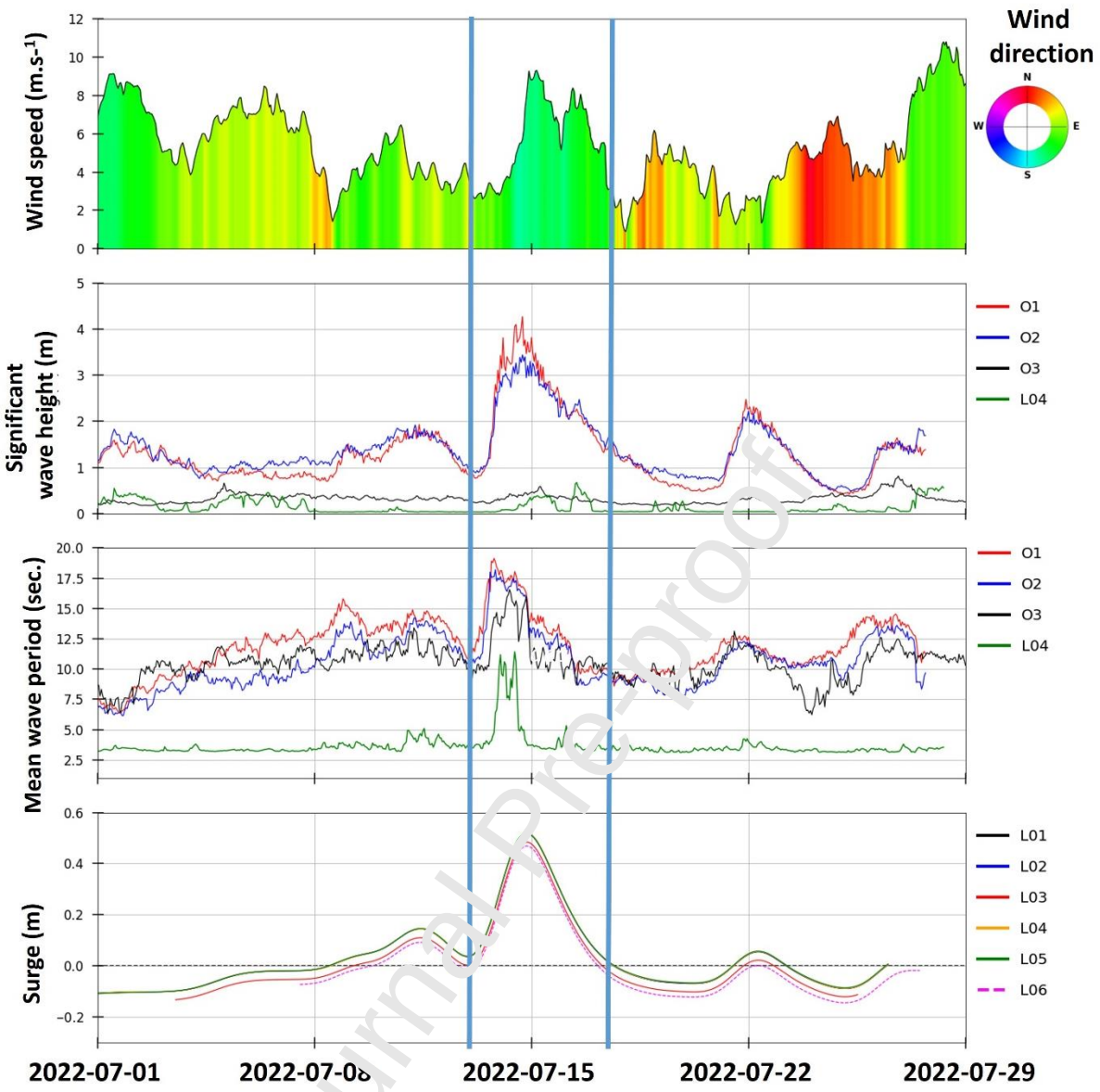

Figure 5: From top to bottom, for the Leg 2: wind ERA5 speeds and directions; significant wave height at the three oceanic stations and the L4 lagoon station; wave period for the three oceanic stations and L4; lagoon surge for the six lagoon stations. All central stations (L01, L02, L04) have the same surge curves as L05 and are overlaid. Blue vertical bars mark the distant swell event around 14th of July. By convention, wind directions indicate where the wind is coming from.

We first note that the 12-16th July distant swell event is clearly visible at Hsig=4.2m in O01, and >3m in O02. Wave periods reached just above 18s in O01 and O02 stations. The O03 station, in the west of the atoll did not receive any high waves during the entire Leg 2. The wind during the event was well established (~7 $m.s^{-1}$) from the south-southeast, hence Hsig in O02, and less importantly O01, is also enhanced by wind and local waves. Lagoon elevation (surge) reaches ~0.5m above the average level for all lagoon sensors. Surges were all synchronous between stations. While the distant swell event quickly reached its highest Hsig, it only very gradually decreased across a 5-day period. We also

note a second more minor wave event peaking at 2.4 m in O01, centered by 22nd July that occurred during much lower wind conditions. It only generated a minimal lagoonal surge, which is inferior to the surge observed around 11th July, a period with lower swell but higher winds.

Current in the passes

Figure 6 provides speeds and directions of the currents in the passes measured on the water column by the three Sentinel ADCP sensors. The major patterns are the two outgoing flows in the two passes (P01, P03) during nearly four days straight at the time of the event. The two passes shift simultaneously in outgoing regime only (Figure 6). The outgoing current speed remains nevertheless modulated by tide. Highest recorded speed reach 1.71 $m.s^{-1}$ (3.3 knots) and 3.3 $m.s^{-1}$ (6.4 knots) respectively in P01 and P03 at mid-depth, hence in the largest, deeper, sections of the passes, where the ADCP were moored. Currents should be certainly stronger in the shallower sections of the passes. Conversely, the velocities recorded in P02, in the lagoon away from the pass but in the jet, remains much lower and directions are also influenced by tide. Outside the distant mega-swell event, the two passes display a classical functioning, with alternant ingoing and outgoing currents modulated by tides. The amount of time the current is going outward or inward the lagoon is different, and these differences can also be explained by moderate waves and wind. These behaviors outside the mega swell event is not the scope of this study and they will be characterized elsewhere. We note however that during the 22nd July more minor wave event (Figure 3), the currents are also mostly outgoing in both passes. This means that the Hsig threshold above which passes are outgoing regardless of the tide should be around 2.2m, if the swell comes from the south.

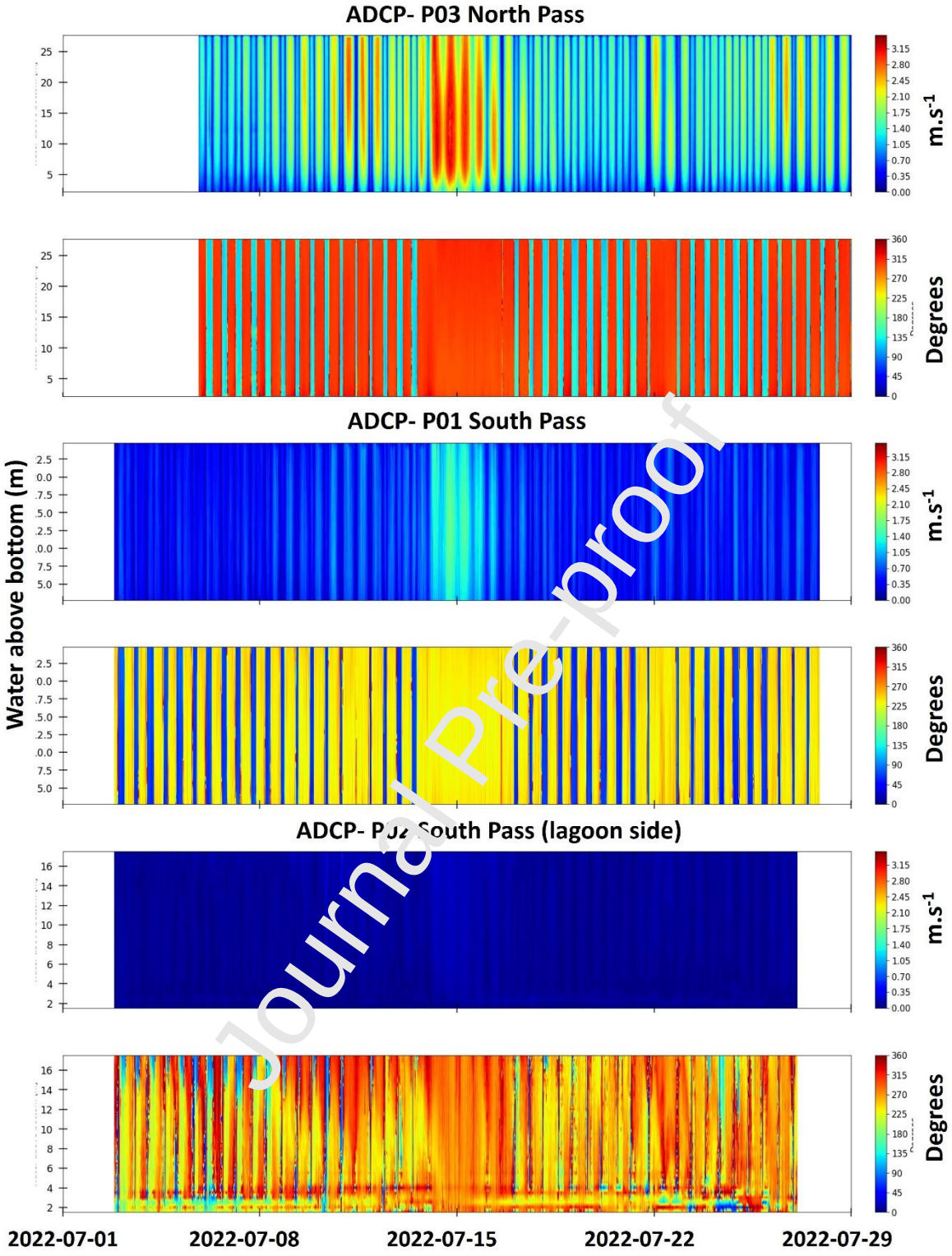

Figure 6: Speeds (in $m.s^{-1}$) and directions (degrees) for the three Sentinel ADCP moored in the passes (P01 and P03) and in the jet lagoonward of the south pass (P02). By convention, directions indicate where the current is going to. Color bars intervals are the same for each sensor for a better comparison.

Current velocities across the atoll rim

The currents through the two southern *hoa* also show a sharp increase in water velocities and levels during the event (Figure 7). Both *hoa* are subjected to strong inflows that remain partially modulated by tide during the event. Outside the event, directions are much more variable, with periods of outgoing flows which seems to be influenced by wind directions, for instance in AQ2 during the north wind period around 25 July 2022.

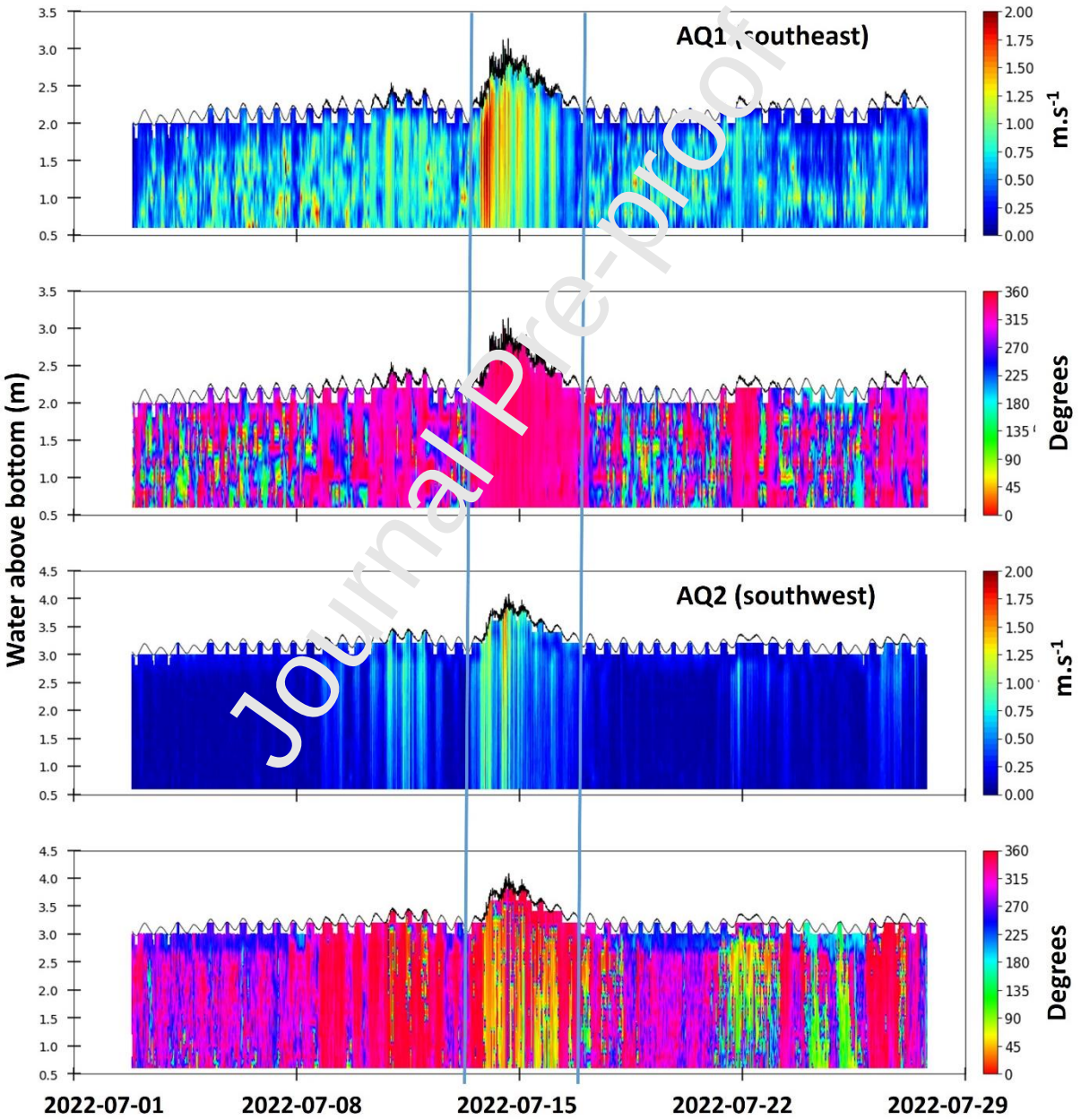

Figure 7: Speeds (in $m.s^{-1}$) and directions measured from the two Aquadopp current meters moored in the south *hoa* (AQ1 and AQ2) during swell event (Leg 2). Black line represents the water level. Blue

vertical bars mark the distant swell event around 14th of July. By convention, directions indicate where the current is going to.

The application of the Aucan et al. (2021) relationships at both daily (Figure 8) and hourly scale (Figure 9) during the Leg 1 and 2 confirmed their ability to predict current velocities in Apataki *hoa*, but best results are nevertheless achieved with a local computation of the coefficients especially for the *hoa* AQ2 (Figure 8). The general equations in Aucan et al. (2021) based on three *hoa* instrumented in Raroia Atoll yields much lower quality results. We also note that results including or not the mega-swell event are of the same statistical quality (Table 2), which confirms the suitability of the Aucan et al. (2021) formulation for high swell conditions that were not met in Raroia.

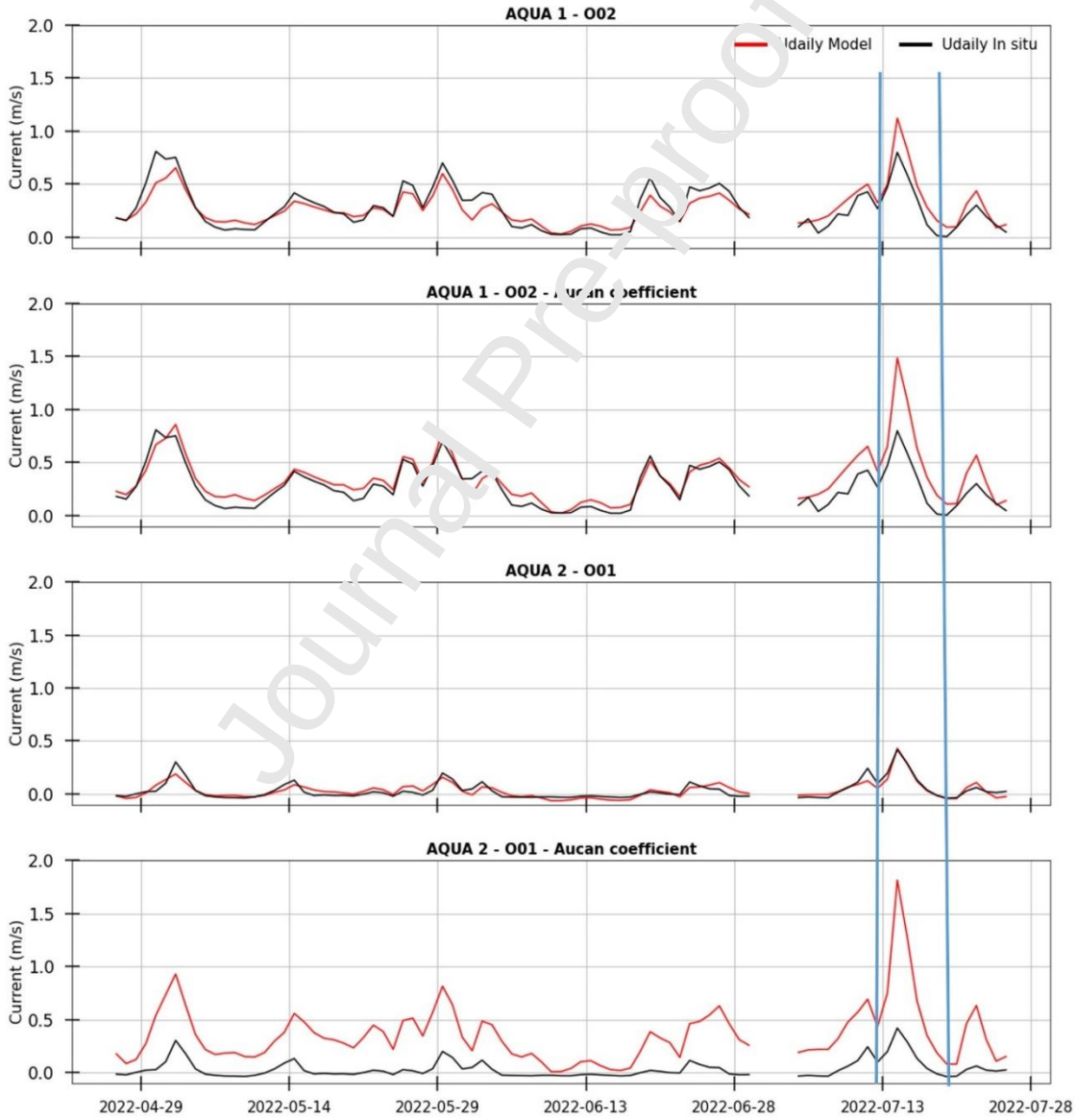

Figure 8: Adjustment of the Aucan et al. (2021) daily-scale relationship between significant wave height (from RBR sensors, see Figure 5) and projected speeds (from Aquadopp sensors, see Figure 7) for the Leg 1 and Leg 2 data on station AQ1 and AQ2. At each station, results are shown when

adjusted with optimized A and C coefficients computed for each *hoa*, and when using the Aucan et al. (2021) general coefficients computed for three Raroia Atoll *hoa*.

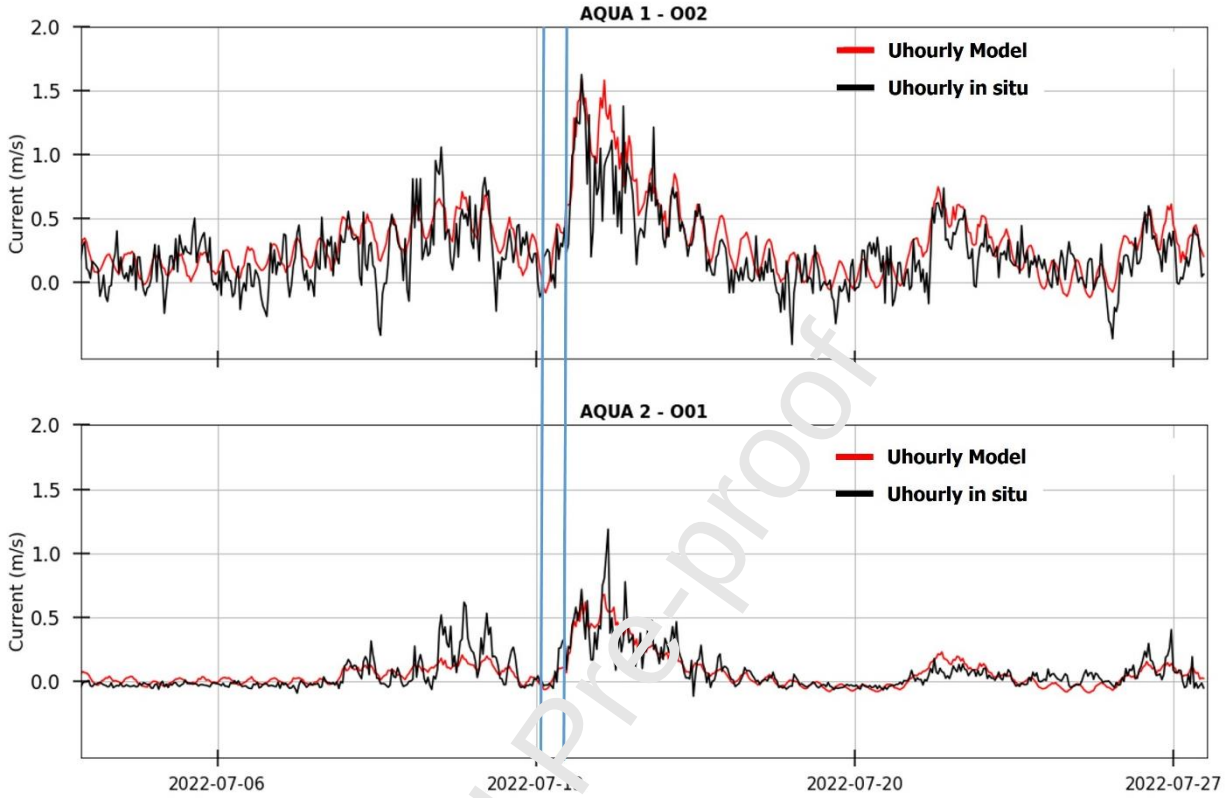

Figure 9: Adjustment of the Aucan et al. (2021) hourly-scale relationship between significant wave height (from RBR sensors, see Figure 5) and projected speeds (from Aquadopp sensors, see Figure 7) for the Leg 2 data on station A1 and AQ2. Results are shown when adjusted with optimized coefficients A, B and C estimated for each *hoa*.

Table 2: A, B & C coefficients from Equation 1 and 2, computed to relate Significant Wave Height with current velocities in hoa AQ1 and AQ2 at daily or hourly scales. Correlation coefficient R and RMSE achieved when comparing modeled vs in situ *velocities. The 'Direction' is the main direction projection. 'Aucan/Raroia' refers to the use of Aucan et al. (2021) most general relationship established form three different hoa of Raroia Atoll. 'Local' stands for a relationship optimized for AQ1 or AQ2.*

	AQ1 Direction=315.4°		AQ2 Direction=41.6°	
Udaily				
	Local	Aucan/Raroia	Local	Aucan/Raroia
A	0.0843	0.113	0.0309	0.113
C	-0.100	0.151	-0.10619	0.151
R	*0.8777*	*0.8777*	*0.9013*	*0.9013*
RMSE	*0.094*	*0.1348*	*0.0364*	*0.3793*
Uhourly				
	Local	Aucan/Raroia	Local	Aucan/Raroia
A	0.112	0.138	0.0374	0.138
B	0.6965	0.427	0.172	0.427

C	-0.231	-0.225	-0.134	-0.225
R	*0.815*		*0.744*	
RMSE	*0.158*		*0.0819*	

Discussion

A summary of Apataki responses to swells and mega-swells

Figure 10 qualitatively summarizes the hydrodynamic functioning of Apataki Atoll in three conditions: A) no wave, B) 'normal' wave, C) mega-swell. Variations in ocean-lagoon exchanges and lagoon levels are shown on the different atoll sectors. Figure 10 helps following the discussion on lagoon level and surge variations on Apataki and Makemo atolls and the factors that have impacted these levels. To discriminate a 'normal', or high, swell versus a mega-swell, no clear definition and threshold limits on significant wave height and periods are provided in the literature. Mega-swells are definitely rare high energy events, but the thresholds between high and mega are not clearly defined. Wave height >5m and period >16s were used by Canavasio (2019) and we kept these values as guidelines, as discussed below. Swell characteristics, for a given event, vary depending on the distance from the source, and a clear definition could therefore rather be based on the characteristics at the source to be unambiguous (Roy et al. 2022). But instead it is often the local context, at the point of impact on a given island that was used to describe a mega swell.

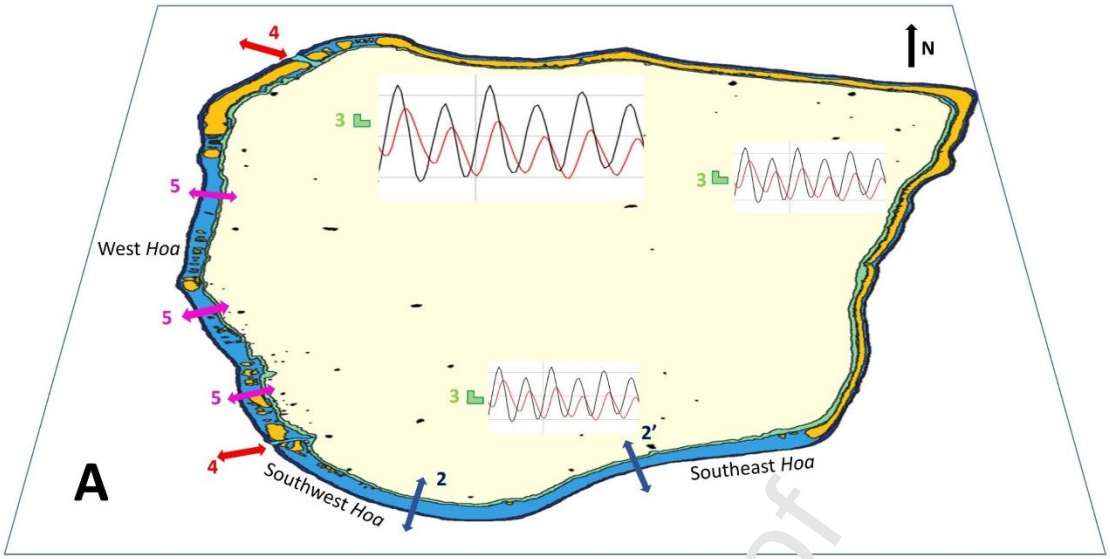

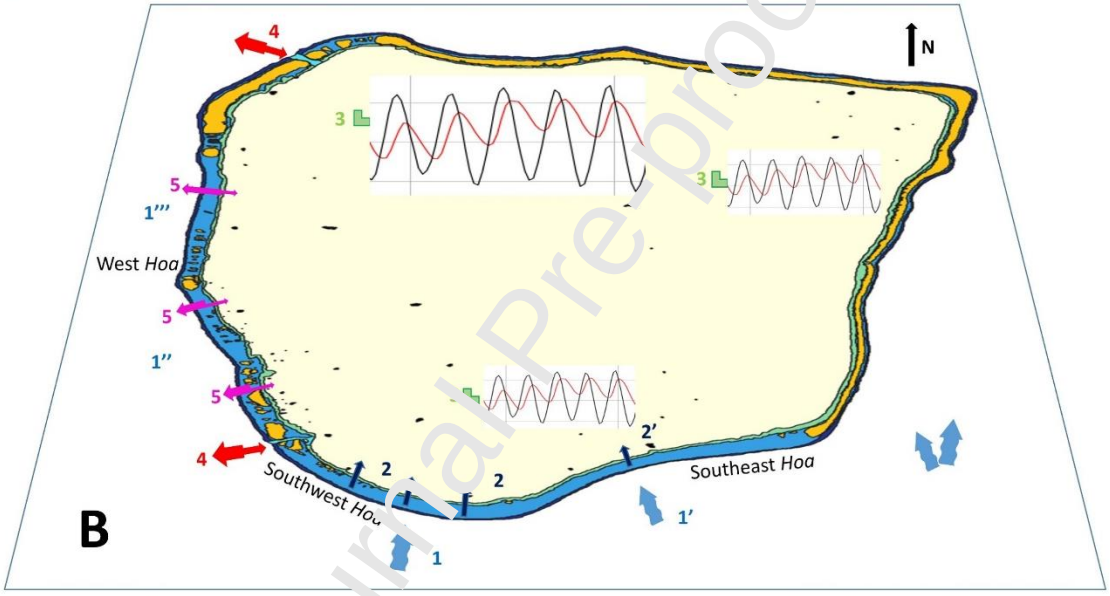

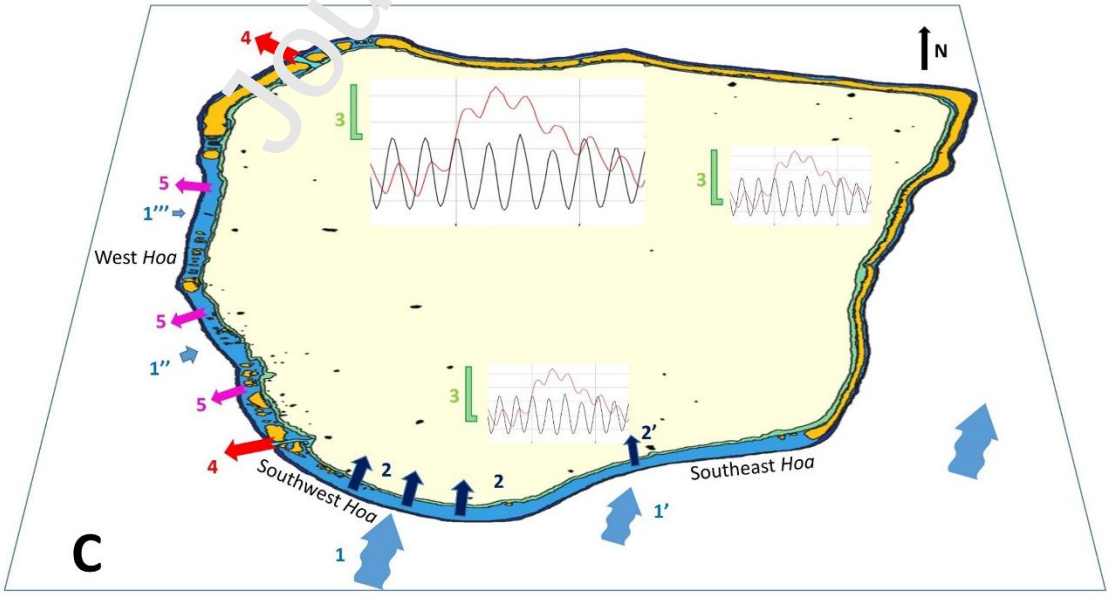

Figure 10: Schematics of ocean-lagoon exchanges and lagoon levels based on swell conditions. Panel A) No swell situation, hence only tide controls the ocean-lagoon exchanges and lagoon levels. Numbers hereafter refer to numbers on the graphs. Specifically, this implies: 1) no incoming waves in all rim sectors; 2) flows in *hoa* are driven by tide in 2, 2' and 5; 3) lagoon levels are modulated by tide, with dephasing and lower amplitude compared to the ocean; 4) outgoing flows through the two deep passes are also driven by tide. Panel B) Situation during 'normal' (low to high) swell, in this case ocean-lagoon exchanges and lagoon levels are controlled by both tide and waves. This implies that: 1) some southern swell may hit the southern rim sectors (southeast or southwest), while other rim sections exposed differently have virtually no incoming waves (as in 1' or 1'''); 2) wave driven flows brings water to the lagoon with flow intensities modulated by tide; 3) lagoon levels increase and are higher than in Panel A) due to wave driven inflows and remain partly modulated by tide; 4) outgoing flows through the two deep passes are still driven by tide, but are also modulated by the flushing of excess water brought in by wave-driven flows, hence outgoing flows become dominant and stronger; 5) outgoing flows through the west side *hoa* not exposed to incoming swells are driven by excess water brought by wave-driven flows, and are still modulated by tide. Depending on the intensity of water flushing in the *hoa* exposed to waves (in 2), outgoing flows become dominant. Panel C) Situation during mega swell, during which ocean-lagoon exchanges and lagoon levels are controlled by waves, implying that 1) south-southwest mega swell hit the southern rim sectors (1, 1'). Other rim sections exposed differently have still very little incoming waves (as in 1'', 1'''); 2) wave driven flows brings water to the lagoon, tide has almost no effect considering the wave-driven flow; 3) lagoon levels reach a maximum due to wave driven inflows with minimal tide influence; 4) outgoing flows through the two deep passes are massively outgoing only, 5) outgoing flows through the west side *hoa* not exposed to incoming swells are driven by excess water brought by wave-driven flows. In all panels, the three similar level curves variations in the lagoon represent that level variations were equal throughout the lagoon. Red and black curves represent lagoon and ocean water levels respectively (see Figure 4).

Differences between 1996, 2011 and 2022 events

Canavasio (2019) characterized the two precedent major distant swell events, in 1996 and 2011. They varied in many aspects, and the 2022 event seems to be more in line with the characteristic of the 1996 swell. One difference is that the 2022 event occurred in Apataki at a time of well-established southeast trade winds (Fig. 5). The Table 3 summarizes the available characteristics of the three events.

Table 3: Characteristics of the three distant mega-swell events since 1996. 1996 and 2011 information from Canavesio (2019). 2022 information from Roy et al. (2022) or from this study. LAT: lower astronomical tide, or lower water level.

Event & location	Wind in atolls	Water elevation or surge	Period during maximum swell height	Origin relative to French Polynesia	Wave height at fetch center	Distance fetch area to Tuamotu	Lowest Pressure at center
July 1996 Makemo	No	2.75 m above LAT	16.8s (WW3)	South	14m	2500 to 3000 km	974 hpa
August	No	1.85 above	18.7s (WW3)	Southwest	18m	5000 to	927 hpa

2011 Makemo		LAT				6000 km	
July 2022 Apataki	Southeast, ~7 $m.s^{-1}$	0.5 m surge	18s (this study)	South	N/A	4500 km	946 hpa

Canavasio (2009) reported a lagoon level rise of 2.85m in 1996, and 1.85m in 2011, measured against the lowest astronomical tide. In Apataki, we observed during the event a maximum lagoon surge of +50cm, which if projected against the LAT as estimated from Leg 1 and Leg 2 (i.e., -0.231m below the average level), could mean a maximum of 0.8 meter elevation, thus almost twice lower than in Makemo 2011. The values reported for Makemo seems very high, but they could also be easily explained by the different geomorphological features between Apataki and Makemo. Indeed, Makemo is an east-west oriented atoll, with a south rim more exposed than Apataki to southern swells due to the absence of other atolls in the south that could block incoming swells. Makemo is also almost asymmetrical in aperture, with all its aperture (*hoa*) in the south, and completely closed in the north. Andréfouët et al. (2005) report for the southern rim of Makemo a degree of aperture of 98%, against 50% in Apataki. Only the two Makemo passes can then efficiently discharge the lagoon when its level rises. Residual *hoa* on the north rim, which are dry most of the time and function only during high swell can also contribute to the discharge (Canavesio 2019). The two atoll lagoons have about the same sizes (around 700 km^2) but overall Makemo is simultaneously more exposed to swell, more open in the south, and less open in the north, all these factors explaining that the surge due to incoming southern swell could reach much larger value in this atoll than in Apataki.

During the 2022 event, Apataki village was flooded in some limited areas (SA, pers. obs.) but not as dramatically as in Makemo, and villagers appeared quite unaffected by the event. According to Damlanian et al. (2013), the Apataki village elevation is between 1m and 2.5m, while the short runway is at about 3m. The 0.5m surge measured during the mega swell when compared to these values explains the low impact of the event in the village. The comparison between Makemo and Apataki confirms that each case can be different. Lagoon side shorelines are also typically of lowest elevation than oceanic sides, hence, lagoon elevation will easily impact lagoon exposed land more prone to inundation. Exposures (or protection) to incoming swells, and geomorphology (lagoon sizes, degree of aperture, distribution of *hoa*) were already characterized (Andréfouët et al. 2022) and could be used as first-order proxy to estimate the vulnerability of each atoll to distant mega-swells. The precise topographic elevation of reef islands hosting critical infrastructures, if available (Damlanian et al. 2013), will permit a fine scale second-order characterization. As of today, precise topographic data are freely and digitally available for a handful of selected atolls (https://www.data.gouv.fr/fr/datasets/base-de-donnees-cartographique-vectorielle/). For instance the main inhabited reef island in Tuamotu, in Rangiroa Atoll, has 72% of its land area lower than 2m altitude, 26% between 2 and 4m, and 2% above 4m. In Hao Atoll which has the second most

populated reef island of Tuamotu, the proportions are remarkably similar to Rangiroa, with 73% (<2m), 26% (2-4m) and 1% (>4m). Note that here, the altitudes are given against the locally measured mean higher high water height of each tidal day (MHHW).

Extreme pass and reef flats currents

The 2022 distant mega-swell event impacting Apataki may not be the more energetic event of the past decades, but the measurements of currents in both passes, and especially in the North Tehere pass are among the highest value ever observed in a Tuamotu atoll pass to our knowledge. Our own measurements in Ahe (Dumas et al. 2012), Raroia (Andréfouët et al. 2023) or Takaroa (Bruyère et al. 2023,) culminated at around 4.8, 5.8 and 4.4 knots (1 knot=0.514 m.s^{-1}) respectively, while here the maximum recorded velocity was 6.4 knots. Measurements in other atolls are scarce, or may not be publicly available if acquired in a military context (for Moruroa or Fangataufa atolls) or for a private contract (Takaroa and Manihi, Takaroa Town Hall, pers. comm.). Several publicly available long time series are nevertheless available, for instance acquired for projects evaluating the hydroelectrical potential of Tuamotu atoll passes. In Hao Atoll, in the southeast Tuamotu, the maximum speed recorded at one point in the Kaki Pass with a Workhorse RDI ADCP moored 10m deep was 7.7 knots the 02/04/2011, 18h31 local time (Marigliano et al. 2011). For the Avatoru Pass in Rangiroa Atoll, Rougerie and Gros (1980) estimated a maximum velocity of 5.8 knots. However, this latter study used two current meters with specifications and type of non-rigid moorings that make them rather unsuitable for the conditions of a Tuamotu atoll pass (one Hydropronics 505 inclinometer and one General Oceanics 2010). Hence the 5.8 knots result from an empirical correction and not from a direct measurement. It may also be well underestimated. In the Tiputa Pass in Rangiroa, Baleilevuka et al. (2013) recorded a maximum speed of 8.9 knots acquired the 27th August 2021, during the 2011 mega-swell first code-red event, using a Nortek AQD current profiler moored 21m deep. This seems to be the highest value ever measured. The maximum speed indicator shows the strength of mega-swell event if used in a long term series, as an indicator of the anomaly. It does not necessarily indicates the highest possible current speed in a given pass. The highest speeds are rather expected to be in the shallowest central part of the pass, generally towards the lagoon entrance, hence not where the current profilers are more often moored.

Besides the maximum speed used here as an indicator of the strength of the mega-swell event, each pass coul be precisely characterized further along its vertical profile using the different ADCP measurement cells (Marigliano et al. 2011) (Fig. 6). Speeds and directions can vary between cells, and

a full characterization of the passes flows, outgoing and ingoing, warrant further investigations for all previously investigated atolls (Ahe, Takaroa, Raroia, and Apataki), especially during normal conditions. This characterization will be presented elsewhere, coupled with hydrobiological profiles (that were not performed at the time of the swell event). Same conclusions arise for the characterizations of the *hoa*. Shallow measurements Figure 7 shows that direction and speed are not homogeneous on the vertical axis, and vary significantly with wind and wave forcing. This has a variety of ecological and biogeochemical implications, when relating the turbulence regime and nutrient uptake across an atoll rim (Atkinson 1992, Pagano et al. 2017).

Possible impacts on population, coastlines and for pearl farming management

Beyond the Tuamotu cases investigated here and in Canavesio (2019), a better understanding of an atoll response to mega-swell events regardless of their origins (distant swell, tropical cyclones, tsunamis) is granted for all atoll regions, even if not all atolls worldwide are exposed to mega-swell occurrences as described in this study. Understanding how lagoon levels will rise and the capacity of a lagoon to flush out waters under the forcing swells is necessary to optimize land developments, and also before considering modifications of the hydrodynamic pathways along the rim. Precautions should not be limited to the area where the swell is incident, but damages can occur at the opposite side of the atoll, as described by Canavesio (2019) in Makemo, and as suggested here in Apataki due to the highest pass current speed, and the level of lagoon surge, in the northern part of the atoll (Figure 5).

Specifically for pearl farming, and also for giant clam farming taking place in the East Tuamotu atoll (Andréfouët et al. 2018), local farmers often call for the enlargement of *hoa* to increase water quality and flows, often after that some algal blooms event have struck benthic or pelagic exploited populations. This idea is however naïve, and does not take into account what may happen in the case of rare high wave events. Artificially enlarged opening will help the inward flushing in normal conditions and outward flushing if they are opposite to incoming swells. This situation can be beneficial. But during big swell event, if they are directly exposed to the incoming swells, enlarged opening will also enhance inward flushing and lagoon surge. As pointed out by Canavesio (2019), distant origin mega-swells in French Polynesia come from the south, but hurricane waves can come from any directions, and in particular west and north (Andréfouët et al. 2012, Laurent and Varney 2014). The impact of these swells is not to be taken lightly, and should call for as much precautions and management decisions enlightened by *in situ* measurements than for the impact of rising seas under global warming. Considering the number of evidences of poor management in Tuamotu atolls

related to the questions of reef island maintenance (it is time to avoid past mistakes (Duvat et al. 2017, 2020b). On the lagoon side, pearl farmers have started to take into account wave events. They rethink their installations to avoid damages due to lagoon level elevation. This includes higher pontoon and working platforms above water, stronger installations, buildings further from the coastline, as well as better monitoring and better attention to warning sent by Météo-France. Some of these measures could be better guided and greatly optimized with adequate knowledge of the hydrodynamic processes driving lagoon elevation in every lagoon.

Acknowledgements

This study was funded by a grant ANR-16-CE32-0004 MANA (Management of Atolls project). Instruments were provided by the Direction des Ressources Marines, OTI project, Contrat de Projet France-French Polynesia, Program 123, Action 2, 2015–2020. We thank our colleagues and divers Yann Follin, Thomas Trophime, Bertrand Bourgeois, Magali Boussion and Caline Basset for their help in the field, as well as Remi Tavaitai for his boat captain skills. The hydrodynamical study of Apataki Atoll was part of the MALIS3 oceanographic cruise on R/V ALIS (https://doi.org/10.17600/18001644). We are grateful to R/V ALIS captain Jean-François 'Jeff' Barazer and all the crew for their skills, dedication and help during the operations.

References

Andréfouët, S., 2013: POLYPERL cruise, RV Alis, https://doi.org/10.17600/13100050

Andréfouët, S., Le Gendre, R., 2022: MALIS 3 cruise, RV Alis, https://doi.org/10.17600/18001644

Andréfouët, S., Ouillon, S., Brinkman, R., Falter, J., Douillet, P., Wolk, F., Smith, R., Garen, P., Martinez, E., Laurent, V., Lo, C., Remoissenet, G., Scourzic, B., Gilbert, A., Deleersnijder, E., Steinberg, C., Choukroun, S., Buestel, D., 2006. Review of solutions for 3D hydrodynamic modeling applied to aquaculture in South Pacific atoll lagoons. Marine Pollution Bulletin 52, 1138–1155. https://doi.org/10.1016/j.marpolbul.2006.07.014

Andréfouët, S., Ardhuin, F., Queffeulou, P., Le Gendre, R., 2012. Island shadow effects and the wave climate of the Western Tuamotu Archipelago (French Polynesia) inferred from altimetry and numerical model data. Marine Pollution Bulletin 65, 415–424. https://doi.org/10.1016/j.marpolbul.2012.05.042

Andréfouët, S., Aucan, J., Jourdan, H., Kench, P., Menkes, C., Vidal, E., Yamano, H., 2015. Conservation of low-islands: high priority despite sea-level rise. A comment on Courchamp et al. Trends in Ecology & Evolution 30, 1–2. https://doi.org/10.1016/j.tree.2014.10.001

Andréfouët, S., Van Wynsberge, S., Kabbadj, L., Wabnitz, C.C.C., Menkes, C., Tamata, T., Pahuatini, M., Tetairekie, I., Teaka, I., Scha, T.A., Teaka, T., Remoissenet, G., 2018. Adaptive management for the sustainable exploitation of lagoon resources in remote islands: lessons from a massive El Niño-induced giant clam bleaching event in the Tuamotu atolls (French Polynesia). Envir. Conserv. 45, 30–40. https://doi.org/10.1017/S0376892917000212

Andréfouët, S., Desclaux, T., Buttin, J., Jullien, S., Aucan, J., Le Gendre, R., Liao, V., 2022. Periodicity of wave-driven flows and lagoon water renewal for 74 Central Pacific Ocean atolls. Marine Pollution Bulletin 179, 113748. https://doi.org/10.1016/j.marpolbul.2022.113748

Andréfouët, S., Bruyère, O., Aucan, J., Liao, V., and Le Gendre, R., 2023. Lagoon hydrodynamics of pearl farming atolls in French Polynesia: the case of Raroia Atoll (Tuamotu Archipelago), SEANOE [data set], https://doi.org/10.17882/94147

Atkinson, M.J., 1992. Productivity of Enewetak atoll reef flats predicted from mass transfer relationships. Continental Shelf Research 12, 799–807.

Aucan, J., Vendé-Leclerc, M., Dumas, P., Bricquir, M., 2017. Wave forcing and morphological changes of New Caledonia lagoon islets: Insights on their possible relations. Comptes Rendus Geoscience 349, 248–259. https://doi.org/10.1016/j.crte.2017.09.003

Aucan, J., Desclaux, T., Le Gendre, R., Liao, V., Andréfouët, S., 2021. Tide and wave driven flow across the rim reef of the atoll of Raroia (Tuamotu, French Polynesia). Marine Pollution Bulletin 171, 112718. https://doi.org/10.1016/j.marpolbul.2021.112718

Baleilevuka,A., Kruger, J., Kumar, S., Turagabeci, M., Damlamian, H., Beg, Z., 2013. Oceanographic Assessment Rangiroa, Kauehi, Arutua, Apataki and Manihi, French Polynesia. SPC SOPAC data release report (PR105)

Bourrouilh-LeJan., F., Tallandier, J., 1985. Sedimentation et fracturation de haute énergie en milieu récifal: tsunamis, ouragans et cyclones et leurs effets sur la sédimentologie et la géomorphologie d'un atoll: motu et hoa, à Rangiroa, Tuamotu, Pacifique SE. Marine Geology 67, 263–333

Bruyère, O., Soulard, B., Lemonnier, H., Laugier, T., Hubert, M., Petton, S., Desclaux, T., Van Wynsberge, S., Le Tesson, E., Lefèvre, J., Dumas, F., Kayara, J.-F., Bourassin, E., Palau, N., Antypas, F., Le Gendre, R., 2022. Hydrodynamic and hydrological processes within a variety of coral reef lagoons: field observations during six cyclonic seasons in New Caledonia. Earth Syst. Sci. Data 14, 5439–5462. https://doi.org/10.5194/essd-14-5439-2022

Bruyère, O., Le Gendre, R., Liao, V., Andréfouët, S., 2023. Lagoon hydrodynamics of pearl farming atolls in French Polynesia: the case of Takaroa Atoll (Tuamotu Archipelago), SEANOE [data set], https://doi.org/10.17882/94146

Canavesio, R., 2015. Estimer les houles cycloniques à partir d'observations météorologiques limitées : exemple de la submersion d'Anaa en 1906 aux Tuamotu (Polynésie française). vertigo. https://doi.org/10.4000/vertigo.15375

Canavesio, R., 2019. Distant swells and their impacts on atolls and tropical coastlines. The example of submersions produced by lagoon water filling and flushing currents in French Polynesia during 1996 and 2011 mega swells. Global and Planetary Change 177, 116–126. https://doi.org/10.1016/j.gloplacha.2019.03.018

Caldwell, P.C., Aucan, J.P., 2007. An empirical method for estimating surf heights from deepwater significant wave heights and peak periods in coastal zones with narrow shelves, steep bottom slopes, and high refraction. J. Coast. Res. 23, 1237–1244. https://doi.org/10.2112/04-0397R.1.

Callaghan, D.P., Nielsen, P., Cartwright, N., Gourlay, M.R., Baldock, T.E., 2006. Atoll lagoon flushing forced by waves. Coastal Engineering 53, 691–704. https://doi.org/10.1016/j.coastaleng.2006.02.006

Damlamian, H., Kruger, J., Turagabeci, M., Kumar, S., 2013. Cyclone wave inundation models for Apataki, Arutua, Kauehi, Manihi and Rangiroa Atolls, French Polynesia. SPC SOPAC Technical REPORT (PR176). Suva, Fiji. 66 p.

Demerliac, A., 1974. Calcul du niveau moyen journalier de la mer. Rapport du service hydrographique de la marine 741, 49–57.

Dumas, F., Le Gendre, R., Thomas, Y., Andréfouët, S., 2012. Tidal flushing and wind driven circulation of Ahe atoll lagoon (Tuamotu Archipelago, French Polynesia) from in situ observations and numerical modelling. Marine Pollution Bulletin 65, 425–440. https://doi.org/10.1016/j.marpolbul.2012.05.041

Dutheil, C., Andréfouët, S., Jullien, S., Le Gendre, R., Aucan, J., Menkes, C., 2020. Characterization of south central Pacific Ocean wind regimes in present and future climate for pearl farming application. Marine Pollution Bulletin 160, 111584. https://doi.org/10.1016/j.marpolbul.2020.111584

Dutheil, C., Jullien, S., Aucan, J., Menkes, C., Le Gendre, R., Andréfouët, S., 2021. The wave regimes of the Central Pacific Ocean with a focus on pearl farming atolls. Marine Pollution Bulletin 162, 111751. https://doi.org/10.1016/j.marpolbul.2020.111751

Duvat, V.K.E., Salvat, B., Salmon, C., 2017. Drivers of shoreline change in atoll reef islands of the Tuamotu Archipelago, French Polynesia. Global and Planetary Change 158, 134–154. https://doi.org/10.1016/j.gloplacha.2017.09.016

Duvat, V.K.E., Pillet, V., Volto, N., Terorotua, H., Laurent, V., 2020a. Contribution of moderate climate events to atoll island building (Fakarava Atoll, French Polynesia). Geomorphology 354, 107057. https://doi.org/10.1016/j.geomorph.2020.107057

Duvat, V.K.E., Stahl, L., Costa, S., Maquaire, O., Magnan, A.K., 2020b. Taking control of human-induced destabilisation of atoll islands: lessons learnt from the Tuamotu Archipelago, French Polynesia. Sustain Sci 15, 569–586. https://doi.org/10.1007/s11625-019-00722-8

Ford, M.R., Kench, P.S., 2015. Multi-decadal shoreline changes in response to sea level rise in the Marshall Islands. Anthropocene 11, 14–24. https://doi.org/10.1016/j.ancene.2015.11.002

Griggs, G., Reguero, B.G., 2021. Coastal adaptation to climate change and sea-level rise. Water 13, 2151. https://doi.org/10.3390/w13162151

Hench, J.L., Leichter, J.J., Monismith, S.G., 2008. Episodic circulation and exchange in a wave-driven coral reef and lagoon system. Limnol. Oceanogr. 53, 2681–2694. https://doi.org/10.4319/lo.2008.53.6.2681

Hoeke, R.K., McInnes, K.L., Kruger, J.C., McNaught, R.J., Hunter, J.R., Smithers, S.G., 2013. Widespread inundation of Pacific islands triggered by distant-source wind-waves. Global and Planetary Change 108, 128–138. https://doi.org/10.1016/j.gloplacha.2013.06.006

Kench, P.S., Brander, R.W., Parnell, K.E., McLean, R.F., 2006. Wave energy gradients across a Maldivian atoll: Implications for island geomorphology. Geomorphology 81, 1–17.

Kench, P.S., Nichol, S.L., Smithers, S.G., McLean, R.F., Brander, R.W., 2006. Tsunami as agents of geomorphic change in mid-ocean reef islands. Geomorphology 95, 361–383. https://doi.org/10.1016/j.geomorph.2007.06.012

Kench, P.S., Ford, M.R., Owen, S.D., 2018. Patterns of island change and persistence offer alternate adaptation pathways for atoll nations. Nat Commun 9, 605. https://doi.org/10.1038/s41467-018-02954-1. https://doi.org/10.1016/j.sedgeo.2017.12.017

Lau, A.Y.A., Terry, J.P., Ziegler, A.D., Switzer, A.D., Lee, J., Etienne, S., 2016. Understanding the history of extreme wave events in the Tuamotu Archipelago of French Polynesia from large carbonate boulders on Makemo Atoll, with implications for future threats in the central South Pacific. Marine Geology 380, 174–190. https://doi.org/10.1016/j.margeo.2016.04.013

Laurent, V., Varney, P., 2014. Historique des cyclones de Polynésie française de 1831 à 2010. Meteo France, Papeete. 172 p.

Magnan, A.K., Ranché, M., Duvat, V.K.E., Prenveille, A., Rubia, F., 2018. L'exposition des populations des atolls de Rangiroa et de Tikehau (Polynésie française) au risque de submersion marine. Vertigo. https://doi.org/10.4000/vertigo.23607

Maragos, J.E., Baines, G.B.K., Beveridge, P.J., 1973. Tropical Cyclone Bebe creates a new land formation on Funafuti Atoll. Science 181, 1161–1164. https://doi.org/10.1126/science.181.4105.1161

Marigliano, D., Taquet, M., Hamlin, J., Levy, P., Soyez, C., Tetaura, N-L. 2011. Etude des courants de la passe Kaki de l'atoll de Hao. Evaluation du gisement hydrolien. Rapport d'étude Ifremer, RBE/RMPF/EMR, Tahiti, 92 p.

Monismith, S.G., 2007. Hydrodynamics of Coral Reefs. Annu. Rev. Fluid Mech. 39, 37–55. https://doi.org/10.1146/annurev.fluid.38.050304.092125

Montaggioni, L.F., Salvat, B., Aubanel, A., Eisenhauer, A., Martin-Garin, B., 2018. The mode and timing of windward reef-island accretion in relation with Holocene sea-level change: A case study from Takapoto Atoll, French Polynesia. Geomorphology 318, 320–335. https://doi.org/10.1016/j.geomorph.2018.06.015

Munk, W. H., and Sargent, M. C. (1948). Adjustment of Bikini Atoll to ocean waves. EOS Trans. Am. Geophys. Union 29, 855–860. doi: 10.1029/TR029i006p00855

Pagano, M., Rodier, M., Guillaumot, C., Thomas, Y., Henry, K., Andréfouët, S., 2017. Ocean-lagoon water and plankton exchanges in a semi-closed pearl farming atoll lagoon (Ahe, Tuamotu archipelago, French Polynesia). Estuarine, Coastal and Shelf Science 191, 60–73. https://doi.org/10.1016/j.ecss.2017.04.017

Pedreros, R., Idier, D., Muller, H., Lecacheux, S., Paris, F., Yates-Michelin, M., Dumas, F., Pineau-Guillou, L., Sénéchal, N., 2018. Relative Contribution of Wave Setup to the Storm Surge: Observations and Modeling Based Analysis in Open and Protected Environments (Truc Vert beach and Tubuai island). Journal of Coastal Research 85, 1046–1050. https://doi.org/10.2112/SI85-210.1

Purkis, S.J., Ward, S.N., Fitzpatrick, N.M., Garvin, J.B., Slayback, D., Cronin, S.J., Palaseanu-Lovejoy, M., Dempsey, A., 2023. The 2022 Hunga-Tonga megatsunami: Near-field simulation of a once-in-a-century event. Science Advances. 9,eadf5493.

Rougerie, F., R Gros, 1980. Les courants dans la passe d'Avatoru, atoll de Rangiroa, archipel des Tuamotu (Notes Doc. Océanogr. No. 80/5(17)). ORSTOM, Papeete.

Roy, A., Martinoni-Lapierre, S., Laurent, V., 2022. Qualification de l'épisode de forte houle du 11 au 14 juillet 2022. Rapport Météo-France, Tahiti, Polynésie française 21 p.

Smithers, S.G, Coral cay classification and evolution, in: D. Hopley (Ed.), Encyclopedia of Modern Coral Reefs: Structure, Form and Process, Springer, Dordrecht, Netherlands, 2011, pp. 237-253

Smithers, S.G., Hoeke, R.K., 2014. Geomorphological impacts of high-latitude storm waves on low-latitude reef islands — Observations of the December 2008 event on Nukutoa, Takuu, Papua New Guinea. Geomorphology 222, 106–121. https://doi.org/10.1016/j.geomorph.2014.03.042

Tartinville, B., Rancher, J., 2000. Wave-Induced Flow over Mururoa Atoll Reef. Journal of Coastal Research 16, 7.

Tolman, H.L., 2009. User Manual and System Documentation of WAVEWATCH III TM Version 3.14. 220p.

Tuck, M.E., Ford, M.R., Masselink, G., Kench, P.S., 2019. Physical modelling of reef island topographic response to rising sea levels. Geomorphology 345, 106833. https://doi.org/10.1016/j.geomorph.2019.106833

Wandres, M., Aucan, J., Espejo, A., Jackson, N., De Ramon N'Yeurt, A., Damlamian, H., 2020. Distant-Source Swells Cause Coastal Inundation on Fiji's Coral Coast. Front. Mar. Sci. 7, 546. https://doi.org/10.3389/fmars.2020.00546

Yamano, H., Kayanne, H., Yamaguchi, T., Kuwahara, Y., Yokoki, H., Shimazaki, H., Chikamori, M., 2007. Atoll island vulnerability to flooding and inundation revealed by historical reconstruction: Fongafale Islet, Funafuti Atoll, Tuvalu. Global and Planetary Change 57, 407–416.

Conflict of Interest

The authors have no conflict of interests.

Highlights

Pacific Ocean atolls are exposed and vulnerable to distant mega-swells

Hydrodynamic conditions in atolls during mega-swells are poorly known

In July 2022, an array of sensors in Apataki atoll captured these conditions

Wave, surge & currents are described before, during & after the event

Surge and damages were limited for Apataki, but remain highly atoll-dependent